Defence Science Journal, Voi. 54, No. 3, July 2004, pp. 293-302

Supersonic Jet Interactions in a Plenum Chamber

K.M. Venugopal, A. Rajkumar, S. Vìjaykant, V. Ramanujachari, and G.C. Pant
Instìtute of Armament Technology, Pune-4ll 025

arni

P.M. Ghanegaonkar
D.Y. Patii College of Engineering, Pune-411 018

ABSTRACT

Understanding thè supersonic jet interactions in a plenum chamber is essential for thè design of hot launch systems. Static tests were conducted in a small-scale rocket motor ioaded with a typical nitramine propellaiit to produce a nozzle exit Mach number of 3. This supersonic jet is made to interact with plenum chambers having both open and closed sides. The distance between thè nozzle exit and thè back piate of plenum chamber are varied from 2.5 to 7.0 times thè nozzle exit diameter. The pressure rise in thè plenum chamber was measured using pressure transducers mounted at different locatìons. The pressure-time data were analysed to obtain an insight into thè flow field in thè plenum chamber. The maximum pressure exerted on thè back piate of plenum chamber is about 25-35 per cent. of thè maximum stagnation pressure developed in thè rocket motor. Ten static tests were carried out to obtain thè effect of axial distance between thè nozzle exit and thè plenum chamber back piate, and stagnation pressure in thè rocket motor on thè flow field in thè open-sided and closed-sided plenum chambers configurations.

Keywords: Plenum chamber, piume flow field, launch tube, launch System, supersonic jet, nozzle exit, flow field, stagnation pressure

1. INTRODUCTION

Most of thè military rockets are launched from launcher tubes. The design of thè launch tube will bave to address thè problems of overpressure and temperature regions due to complex piume flow field-sided downstream of thè nozzle and ìts interactìon with thè confining side walls. Bouslog[1], *et al.* carried out simulated tests of under-expanded exhaust plumes (accelerated unheated high pressure air) impinging on thè face of multitube launcher assembly and concluded that for a given nozzle-launcher configuration, thè ratio between thè piume diameter and thè launch tube diameter was a function of stagnation pressure and thè separation distance between thè nozzle exit piume and thè launcher. Korst and Bertin[2] developed an engineering mode! to describe thè flow field which was produced when an under-expanded supersonic nozzle exhausted into a Constant area tube and found reasonable agreement between theory and experiments[3] in thè impingement region. Rocket launchings were conducted by Bertin and Batson[4] to obtain a quantitative understanding of thè constrictive step-launcher tube flow field. They

Revised 18 March 2003

found a strong reverse (blow by flow) when thè exit piane of thè nozzle crossed thè constriction in thè launcher tube. Cold gas and double-base solid propellant static rocket tests were conducted in thè launcher tubes by Batson and Bertin[5] to obtain thè wall pressure distribution. They concluded that thè base pressure depends on thè total pressure and that thè flow in thè launcher tube is a function of thè ratio of base pressure to thè total pressure. Marongin[6], *et al.* studied thè non-steady piume wall interactions in rocket launch tubes through simulated air flow and water table experiments and obtained useful information on peak pressure and cycle frequencies.

The present work on supersonic jet interactions in a plenum chamber is motivated due to (i) an urgent requirement to launch powerful rockets from lightweight launchers, (ii) when thè exhaust gases from a rocket, ie, exiting from a given launch tube impinge on thè face of thè launcher assembly, a portion of thè impinging flow splash back leading to thè change in free-flight trajectory of thè rocket, and (iii) identification of peak pressure regions exerted in thè plenum chamber and thè launch tube, leading to a better structural design of thè launcher.

The objective of thè present study is to experimentally determine thè static pressures exerted on thè walls of thè duct and thè plenum chamber by thè supersonic flow exhausting from thè nozzle by burning a typical nitramine propellant in thè rocket motor. The distance between thè nozzle exit and thè plenum chamber base piate is varied to simulate thè conditions of thè rocket movement inside thè launcher tube. The exhaust gases are handled in two different ways-through open-sided and closed-sided plenum chamber. In thè open-sided plenum chamber configuration, thè gases tura by 90° to exit to thè atmosphere. In thè closed-sided plenum chamber configuration, thè gases tura through 180° and exit through an uptake to thè atmosphere.

2. EXPERIMENTAL SETUP

To study thè effect of supersonic piume impingement on thè back piate of open-sided and closed-sided plenum chamber configuration, static rocket motor firings into a suitably instrumented open-sided and closed-sided plenum chamber, having provision for pressure measurement are carried out. The hardware setup consists of thè following:

a) A scaled test solid rocket motor was mounted on a lathe. The solid rocket motor is a standard ballistic evaluation motor of inner diameter 90 mm; length 120 miri and thickness 20 mm made of stainless steel to withstand a maximum chamber pressure of 150 bar. The rocket motor nozzle is designed to produce an exit Mach number of 3. The exit and thè throat diameters of thè nozzle are 24.3 mm and 9.6 mm, respectively to arrive at thè exit-to-throat area ratio of 6:4. The semi cone angles of thè nozzle convergent and divergent sections are 15° and 13°, respectively. The propellant used in this study is a nitramine propellant consisting of nitrocellulose (54 %), nitroglycerine (39 %), RDX (5 %) and carbamite (2 %). The inner and thè outer diameters of thè propellant grain for ali thè static tests are 66.4 mm and 9.6 mm, respectively. The ignition was provided by burning a pyrotechnic mixture through an electrically initiated squib.

b) The open-sided or closed-sided plenum chambers were mounted on thè lathe carriage with provision made for tapping pressure on thè back piate and thè other locations in thè test article.

e) Pressure transducer was mounted on thè rocket motor.

d) Instrumentation for thè measurement of temperai variation of pressure. This consists of strain gauge transducers, a 16-channel data acquisition System, a personal computer installed with data acquisition software, a visual designer™, and a data acquisition card.

The static tests were carried out in a room with reinforced concrete walls. A window with 25 mm thick bulletproof safety glass was provided on thè wall separating thè test room from thè control room. The electrical connections were also made fireproof. A small opening was provided for routing of a transducer and igniter cables. A control room is used to control ali thè operations of thè test firing.

2.1 Plenum Chamber with Open Sides

The exhaust piume from thè nozzle exit, situated inside thè canister duct, enters thè plenum chamber. The canister duct is made of mild steel plates of 16 mm thick and is welded to thè plenum chamber, also made of mild steel plates of 16 mm thick. The plenum chamber is open to thè atmosphere on both th& sides. Therefore, thè gases exhausted from thè nozzle travel straight, impinge on thè back piate of thè plenum chamber and turn by 90° to mix with ambient air as shown in Fig. l.

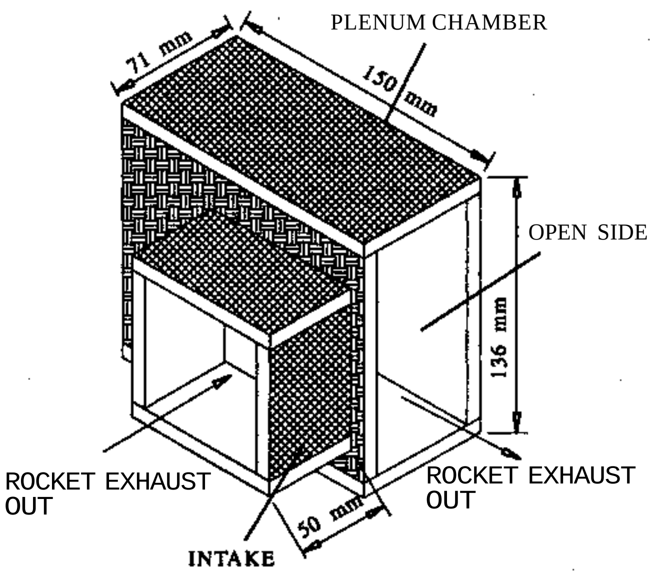

Figure 1. Schematic of plenum chamber assembly with open sides.

Ten pressure tapings are located within a diameter of 50 mm in thè impingement region on thè back piate. The radiai distribution of these with thè centre taping located on thè nozzle axis is shown in thè Fig. 2. Two tapings are located on thè duct and thè one is placed on top of thè plenum chamber, midway between thè plenum chamber walls and in line with thè centre of thè canister duct.

2.2 Plenum Chamber with Closed Sides

The exhaust piume from thè nozzle exit enters thè plenum chamber through thè intake of thè

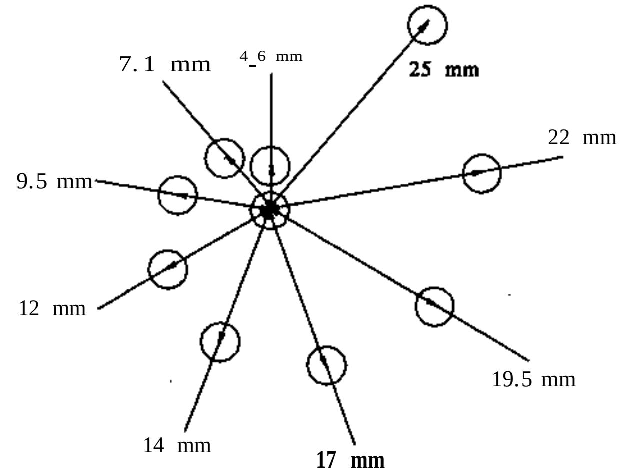

Figure 2. Pressure tappings on impingement piate

canister. The plenum chamber is made of mild steel plates of 8 mm thick, welded together to form thè hardware assembly. The assembly consists of an intake passage, a plenum chamber, and an uptake passage as shown in thè Fig. 3. Ten transducers

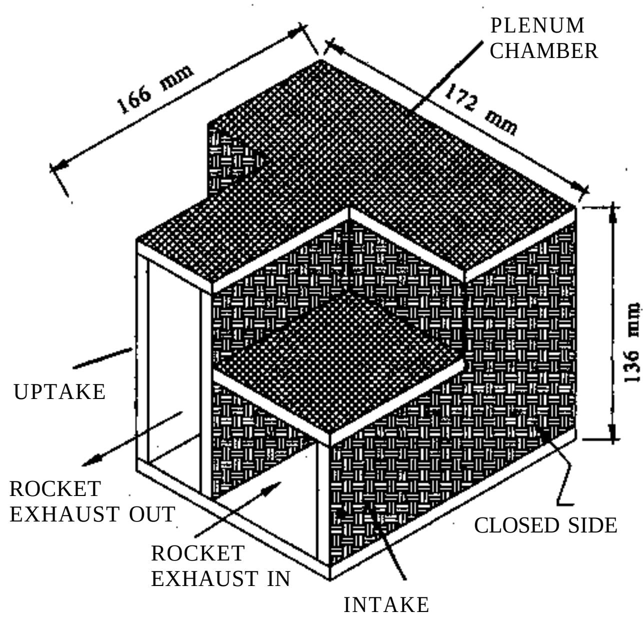

Figure 3. Schematic of plenum chamber assembly with closed sides.

are located within a diameter of 100 mm in thè impingement region on thè back piate of thè plenum chamber. The radiai distribution of these is shown in thè Fig. 4. One transducer each on thè enclosed sides of thè plenum chamber, one on thè intake

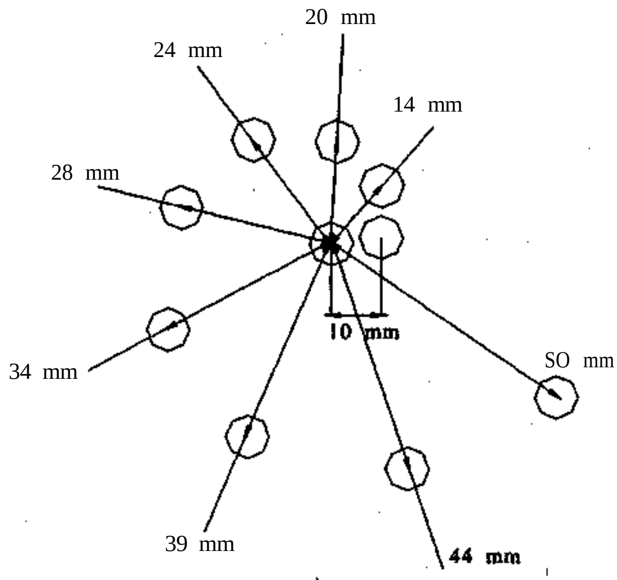

Figure 4. Pressure tappihgs on impingement piate

passage, and two on thè uptake passage, are provided for thè pressure measurement. Plenum chamber is fixed on a base piate of 8 mm thickness mounted on a special fixture made on thè lathe carriage. With this arrangement, it is possible to move thè plenum chamber assembly in x and y directions and thus, align it with thè centreline of thè rocket motor nozzle.

3. RESULTS & DISCUSSIONS

Static tests were carried out to obtain thè pressure distributiòn in thè impinging region of thè plenum chambers. It is reported[7] that thè impinging free jet has complicated flow elements, consisting of a barrel shock, a exhaust gas jet boundary, a Mach disk, a contaci surface, a reflected shock, a piate shock, a sub-tail shock and a stagnation bubble as depicted in Fig. 5. Pive static tests each

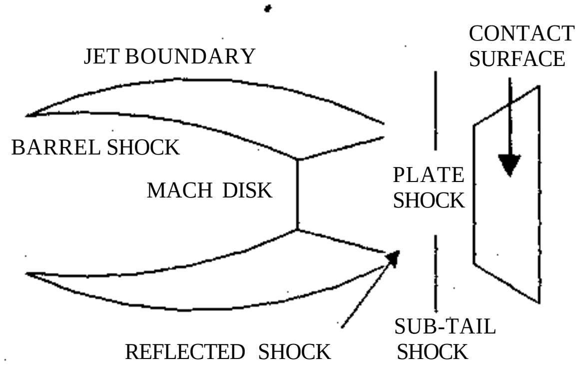

Figure 5. Schematic sketch of impinging jet

with both thè open-sided and thè closed-ended plenum chambers were carried out to get an insight into thè flow field.

3.1 Plenum Chamber with Open Sides

The rocket piume impingement phenomena have been studied by conducting five static firings, using thè nitramine-based propellant, by keeping thè nozzle exit piane at 2.5D, 3D, 4D, 5D and 6D (D is thè nozzle exit diameter) distances from thè fully instrumented impingement piate of thè plenum chamber. The centreline of thè canister intake duct and thè nozzle axis are matched, thereby, ensuring that thè impingement surface is at 90° to thè jet exiting thè nozzle.

3.1.1 *Effect of Axial Distane?*

To obtain thè effect of axial distance on thè flow field, thè transient pressure data collected during thè static tests are plottèd along thè radiai distance of thè plenum chamber impingement region at a chamber pressure (P_c) of 45 bar and at a nozzle exit mass flux of 335 kg/m^{2}s. Two axial distances *(x)* between thè nozzle exit piane and thè back piate of plenum chamber, such as *x/D* = 3 and 6 are considered. Figure 6 shows thè

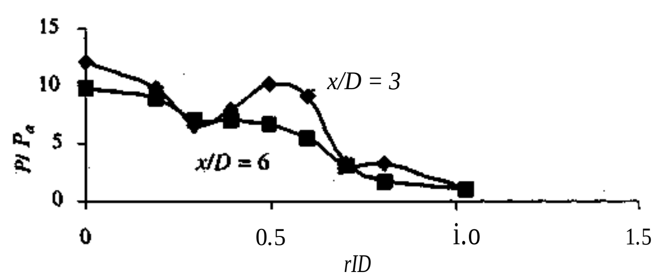

Figure 6. Radiai pressure distributiòn (P_c = 45 bar)

radiai pressure distributions nondimensionalised by thè ambient pressure P_a at thè axial distances corresponding to *x/D* = 3 and 6. The symbol r is thè radiai distance. It is seen that thè pressures exerted on thè impingement region, coinciding with thè nozzle axis, are maximum at 12 bar and 10 bar for *x/D* = 3 and 6, respectiyely. The pressure registered is more at shorter axial distance. The pressure distributiòn patterns for both thè axial distances are not identical. After a decrease in pressure from thè maximum value at thè centre, a steep rise is noted at x/D = 3 around r/D = 0.5 and no rise for x/D = 6. At a smaller distance (x/D = 3), thè centreline pressure is maximum due to strong piate shock and thè next steep increase of pressure at r/D = 0.5 is likely to be thè result of thè interaction between thè piate shock and thè reflected shock. Further, there is a continuous decay of pressure along thè radiai direction in view of thè flow through thè open duct to thè atmosphere. At a longer axial distance (x/D = 6), after an initial increase of pressure on thè centreline to about 10 bar due to a strong piate shock, thè pressure in thè radiai direction decreases continuously, duplicating thè characteristics of a subsonic jet. This could be due to thè predominant effect of mixing of thè jet over shock interaction at larger distances between thè nozzle exit and thè back piate of thè plenum chamber. Figure 7 shows thè radiai pressure variation (30 bar) for thè plenum

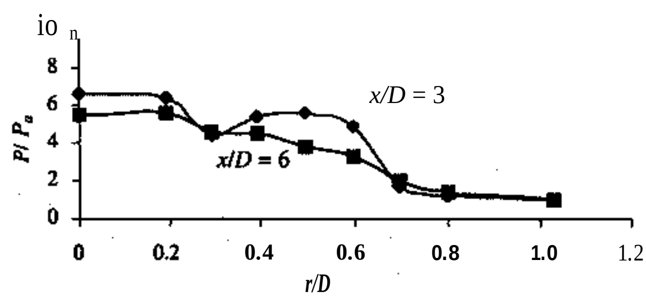

Figure 7. Radiai pressure distribution (P_c = 30 bar)

chamber. The variations are similar except thè changes in thè magnitudes of thè pressure. The pressures exerted on thè top of thè plenum chamber and thè canister inlet are nearly equal to thè atmospheric pressure.

3.1.2 *Effect of Chamber Pressure*

The combustor pressure is vital to thè determination of thè flow field. From thè pressure-time traces of thè static tests, impingement piate pressure data are extracted for different stagnation pressures of thè combustor and replotted. Figure 8 shows thè radiai distribution of pressure on thè impingement piate for two different combustor stagnation pressures, such as 45 bar and 30 bar, keeping thè back piate at an axial distance of x/D = 3 and at an average mass flux of 335 kg/m^{2}s.

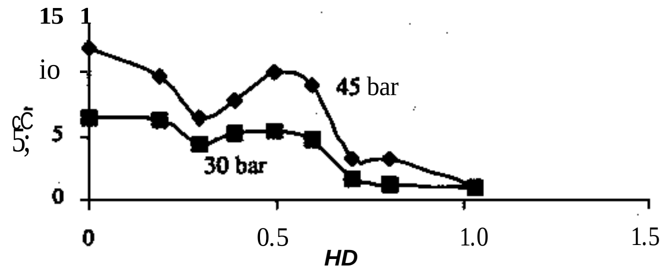

Figure 8. Radiai pressure distribution (x/D = 30 bar)

The stagnation pressure of 45 bar corresponds to thè near-adapted nozzle situation and 30 bar corresponds to thè over-expanded nozzle condition (ratio of nozzle exit pressure to ambient pressure is about 0.7) of thè nozzle. It is evident from thè Fig. 8 that thè lesser chamber pressure gives rise to lesser impingement pressure. The variation of radiai pressure is identical for both thè chamber pressures. It is obvious that thè shock patterns and thè subsequent variations in pressure are basically affected by thè supersonic nozzle exit Mach number, which is about 3.0. After a drop in pressure, there is a sharp increase in pressure around r/D = 0.5, indicating thè likelihood of thè interaction of piate shock with thè reflected shock downstream of thè Mach disc away from thè centreline coinciding with thè nozzle axis. Figure 9 shows thè radiai pressure distribution at an axial distance corresponding to x/D = 6 at thè chamber pressures of 45 bar and 30 bar. Though thè chamber pressure variation changed thè magnitude of thè-pressure exerted on thè impingement piate, thè overall pattern is similar. This strengthens thè argument that so long as thè nozzle exit Mach number is supersonic and nearly thè same, thè shock patterns and thè subsequent pressure variations remain thè same. As thè axial distance corresponding to x/D = 6 is far away as compared to x/D = 3, thè total shock structure got changed, resulting in different pattern of radiai pressure distribution.

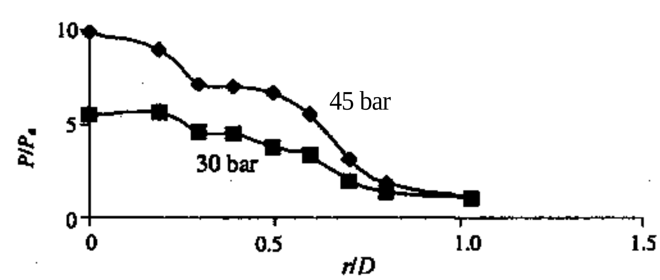

Figure 9. Maximum radiai pressure distribution (x/D = 6)

3.1.3 *Maximum Radiai Pressure Distribuitoti*

To consolidate thè impingement piate pressure data and to find thè maximum possible pressure loads exerted on thè piate, thè maximum pressure values are extracted from thè pressure-time traces and replotted in thè Fig. 10.

The Consolidated data are shown in Table 1. The maximum pressure as a percentage of thè maximum combustor pressure is between 23-29 per cent for a variation of axial distance *(x/D)* between 2.5 to 6.0. The nozzle exit average mass flux variation is between 333-347 kg/m^2s. This is a very useful input to thè structural designer of thè plenum chamber.

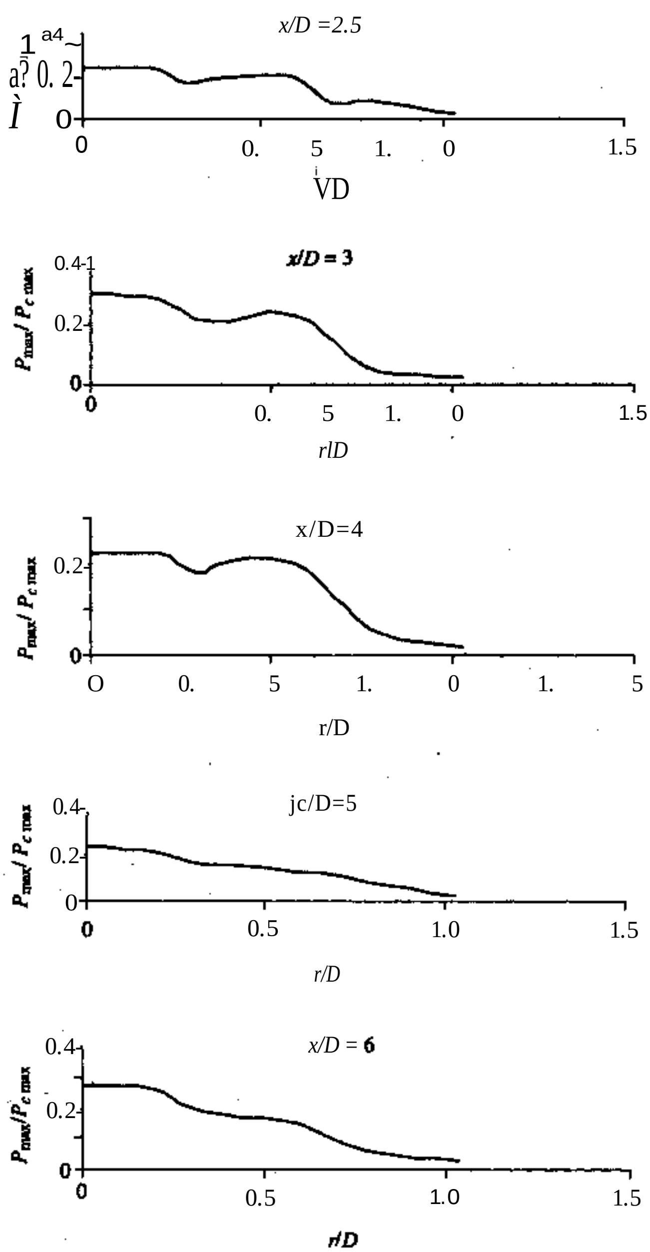

Figure 10. Maximum radiai pressure distribution

Table 1. Performance parameters (open-sided plenum chamber)

x/D	Grain configuration	Time of burning (s)	Average nozzle exit mass flux (kg/m^2s)	Max. impingement pressure as a percentage of max. chamber pressure generated
2.5	L = 38.7 mm M = 212.8 g	1.378	333	25
3.0	L = 40.1 mm M = 220.9 g	1.421	335	29
4.0	L = 41.5 mm M = 226.3 g	1.408	347	23
5.0	L = 40.1 mm M = 221.1 g	1.422	335	23
6.0	L = 39.8 mm M = 220 g	1.409	337	27

It is seen that thè maximum pressure is exerted on thè back piate of thè plenum chamber along thè axis of thè nozzle. The radiai pressure variations under ali axial distances are almost similar. There is a drop in pressure initially, followed by an increase and decrease of pressure towards thè edge of thè jet. The tendency for thè increase of pressure away from thè centre is noted for lower axial distances corresponding to *x/D* = 2.5 to 4. For *x/D* = 5 and 6, thè pressure dropped continuously indicating a free jet behaviour. The pressure variations are basically due to multiple shock interactions in thè impingement region. In ali these tests, thè region of appreciable pressure variation is over a radiai distance of about 0.75 times thè nozzle exit diameter. This implies that thè additional strengthening is needed for this region, which is taking up thè majority of thè pressure and heat loads during thè static test.

3.2 Plenum Chamber with Closed Sides

The results obtained in thè five static tests with closed sides of thè plenum chamber are discussed here. The distance between thè nozzle exit piane and thè impingement region of thè plenum chamber is varied in these tests. The corresponding nondimensional distances, nondimensionalised by thè exit diameter of thè nozzle are 3D, 4D, 5D, 6D, and 7D. The pressure measurements are carried out on thè impingement region of thè plenum chamber, intake and uptake passages.

3.2.1 *Effect of Axial Distance*

The static test data obtained at various locations on thè back piate of thè plenum chamber are plotted in thè Fig. 11 at two axial distances, such as *xlD - 4* and 7, keeping thè combustion chamber pressure and mass flux Constant at 50 bar and 400 kg/m^{2}s, respectively.

The volume of thè plenum chamber is sufficiently large that thè pressure exerted on thè side walls of thè plenum chamber, uptake and canister inlet are nearly atmospheric. This implies that thè flow field characteristics are nearly thè same as that of thè open-sided plenum chamber. From thè video recordings, it is seen that thè flow exited through thè canister intake passage also apart from thè uptake passage. This is known as blow by flow[4], which is detrimental to thè movement of thè rocket inside thè canister. Blow by flow is thè reversai of thè flow between thè rocket motor nozzle and thè canister tube. The supersonic exhaust piume impinges on thè wall at a short distance downstream of thè exit piane, creating an impingement shock wave. When thè shock wave is of thè larger strength, thè entrained air and thè part of thè piume flow do not have enough momentura io pass through thè shock, and hence, turn upstream and flow out of thè canister tube. It is seen that thè pressure exerted on thè impingement region coinciding with thè nozzle axis are maximum about 12.5 bar and 9.5 bar *forx/D = 4* and 7, respectively. The pressure exerted is more at lesser axial distance. The pressure distribution patterns for both thè axial distances are not similar. For *xlD* = 4, a sharp decrease of pressure is noted till *rID* = 0.7 and a small increase and decrease of pressure thereafter. For *xlD* = 7 (after a sharp decrease up to *rID* = 0.5), thè pressure increased and decreased towards thè edge of thè jet. Figure 12 shows thè radiai pressure distribution at a combustion chamber pressure of 40 bar for two different axial distances corresponding to *xlD* = 4 and 7. The mass flux is kept same at 400 kg/m^{2}s.

In this case also similar trends are noted. The maximum pressures of 9.5 bar and 5.5 bar got registered on thè centreline for *xlD = 4* and 7, respectively. After a steep decrease in pressure along thè radiai direction, increase of pressure occurred at *rID* = 0.5 for *xlD = 1* and at *rID* = 0.9 for *x/D = 4.* The possible reason for thè above phenomenon could be thè occurrence of recompression shocks at short axial distances after a strong piate shock, whose strength decreases along thè radiai distance. More insight needs to be obtained using computational fluid dynamics and flow-visualisation techniques.

3.2.2 *Effect of Chamber Pressure*

The stagnation pressure in thè combustion chamber is important in thè determination of thè nozzle exit flow field. Figure 13 shows thè radiai distribution of pressure on thè impingement piate

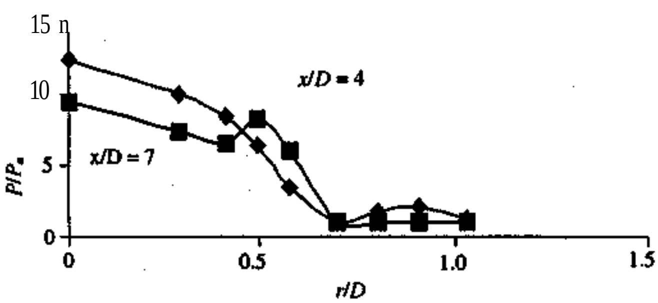

Figure 11. Radiai pressure distribution (P_c = 50 bar)

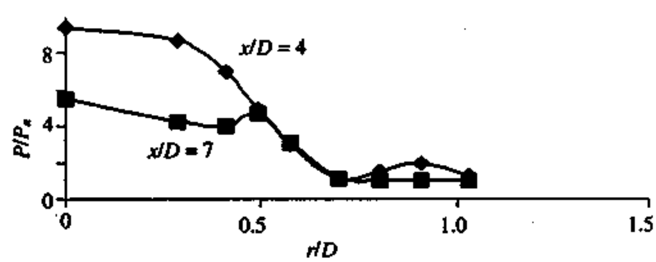

Figure 12. Radiai pressure distribution (P_c = 40 bar)

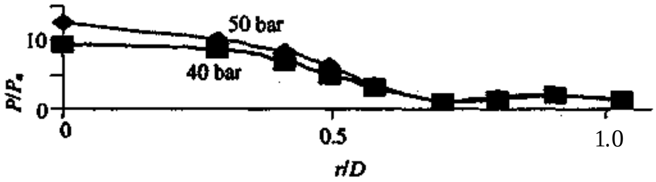

Figure 13. Radiai pressure distribution *(x/D* = 4)

for two different combustor stagnation pressures, such as 50 bar and 40 bar, keeping thè back piate at an axial distance corresponding to *x/D* = 4 with a Constant mass flux of 400 kg/m^{2}s.

The stagnation pressure of 50 bar corresponds to slightly under-expanded condition and thè condition is over-expanded, with a pressure ratio of about 0.86, for thè stagnation pressure of 40 bar. It is seen that thè lower qhamber pressure gives rise to thè lower pressure on thè impingement region. The radiai pressure variations are identical for both thè stagnation pressures, indicating thè fact that thè shock patterns of thè supersonic jet flow are decided by thè jet exit Mach number, which is about 3 and Constant under ali thè conditions. Similar variations are noted in thè Fig. 14, showing thè axial distance corresponding to *x/D* = 7.

3.2.3 *Maximum Radiai Pressure Distribution*

The impingement region pressure data is Consolidated to bring out thè maximum pressure loads impacted on it. Figure 15 shows thè variation of thè maximum pressures obtained in various pressure channels nondimensionalised by thè maximum combustion chamber pressure as a function of nondimensional radiai distance, nondimensionalised by thè nozzle exit diameter, in thè plenum chamber

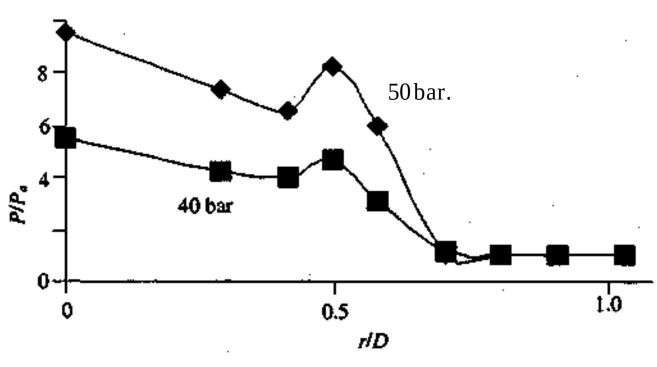

Figure 14. Radiai pressure distribution *(x/D* = 7)

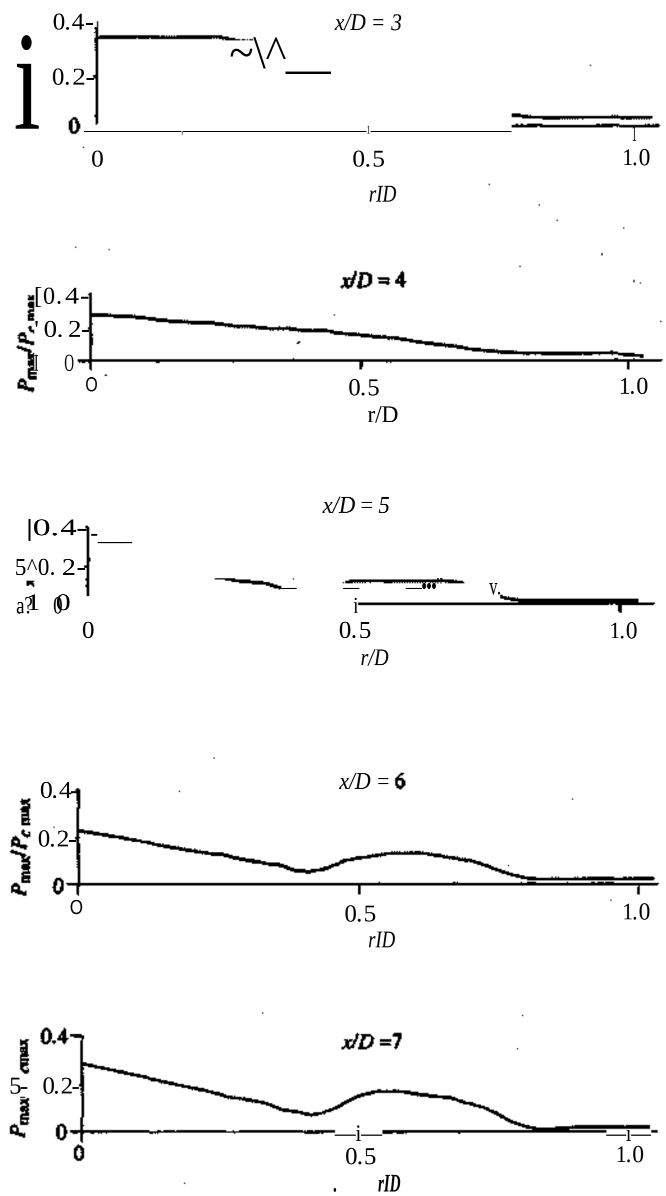

Figure 15. Maximum radiai pressure distribution

impingement region. A reversai of thè trend in pressure distribution compared to that depicted in thè Fig. 10 for thè open-sided plenum chamber is noted. The maximum pressures have sharply fallen for smaller axial distances corresponding to *x/D* = 3 and 4. For axial distances corresponding to *x/D* = 5 to 7, there is a tendency for thè radiai pressure to increase around *r/D* = 0.6, and then falL This indicàtes a clear change in thè shock interactions having stronger recompression shocks for thè close-sided plenum chamber at larger separation between thè nozzle exit and thè back piate of thè plenum chamber. The Consolidated data are shown in thè Table 2.

Table 2. Performance parameters (closed-sided plenum chamber)

xlD	Grain configuration	Timeof burning (s)	Average nozzleexit mass flux (kg/m^{2}s)	Max. impingement pressure as a percentage of max. chamber pressare generateti
3	L = 40.8 mm M = 222.7 g	1.387	346	34
4	L = 52.7 mm M = 291.05 g	1.562	401	28
5	L = 50.3 mm M = 276.7 g	1.562	382	23
6	L = 52.8 mm M = 289 g	1.536	418	23
7	L = 52.7 mm M = 285.2 g	1.559	394	28

The maximum pressure as a percentage of thè maximum combustor pressure is between 23-34 per cent for a variation of axial distances corresponding to *xlD* between 3 to 7. The nozzle exit mass flux variation is between 346-418 kg/m^{2}s. This input is an important one for thè structural designers. In ali these static tests, thè region of appreciable pressure variation is over a radiai distance of about 0.75 times thè nozzle exit diameter.

4. CONCLUSIONS

The following conclusions are arrived at, based on thè experimental investigations on supersonic jet flow under two different plenum chamber configurations.

4.1 Open-sided Plenum Chamber Experiments

- The maximum impingement pressure is registered on thè centreline joining thè axis of thè nozzle and thè plenum chamber.
- It is seen that thè percentage of maximum impingement pressure exerted is about 23-29 per cent of thè maximum pressure generated in thè rocket motor combustion chamber.
- It is observed in ali thè static tests that thè region of appreciable pressure variation on thè impingement surface of plenum chamber is over a radiai distance of about 0.75 times thè nozzle exit diameter around thè nozzle canister duct centrai axis.
- The supersonic flow interactions are too complex to be clearly identified and understood. The present experimental results can be better explained with thè help of computational fluid dynamics and flow visualisation techniques.

4.2 Closed-sided Plenum Chamber Experiments

- Measurement of pressure at various locations on thè intake, plenum chamber, uptake, and rocket motor gave insight into thè flow phenomena. The maximum pressure exerted by thè supersonic piume on thè impingement region was about 23 to 34 per cent of thè maximum rocket chamber pressure. The region of appreciable pressure variation is over a radiai distance of about 0.75 times thè nozzle exit diameter.
- The pressure exerted on thè intake, uptake, and closed sides of thè plenum chamber are near atmospheric values.
- It is concluded that thè impingement region of thè plenum chamber is a criticai region requiririg reinforcement and thè other parts are safe from pressure loads. This is a very important input to thè structural designers of thè launch tubes.

ACKNOWLEDGEMENT

The authors are grateful to thè Rear Àdm A.K. Handa, Director & Dean, Institute of Armament

Technology, Fune and Dr V.K. Saraswat, Programmo Director, PGAD, Hyderabad, for their encouragement to carry out this work. The authors are indebted to Dr Haridwar Singh, thè then Director, High Energy Materials Research Laboratory, Fune, for providing solid propellant grains for conducting thè tests. The help rendered by sarvashri J.C Thomas, N. P. Mule and Anil. Gawade in carrying out thè experiments is sincerely acknowledged.

REFERENCES

1. Bouslog, S.A.; Bertin, J.J. & Wingert, W.B. Flow field produced by rocket exhaust impingement of a multiple launcher. *J. Spacecraft Rockets,* 1984, 21(4), 323-29.
2. Korst, H.H. & Bertin, J.J. Analysis of secondary flow for tube-launched rocket configuration. *J. Spacecraft Rockets,* 1983, 20(1), 35-42.
3. Bertin, J.J.; Idar, E. & Broker, D.L. Secondary flows in a rocket launcher tube. *J. Spacecraft Rockets,* 1981, 18(2), 119-26.
4. Bertin, J.J. & Batson, J.L. Experimentally determined roeket-exhaust flow field in a constrictive tube launcher. *J. Spacecraft Rockets,* 1975, 12(12), 711-17.
5. Batson, J.L. & Bertin, J.J. Rocket exhaust flow in tube launchers. /. *Spacecraft Rockets,* 1974, 11(11), 739-40.
6. Marongin, M.J.; Korst, H.H. & White, R.A. Non-steady piume wall interactions in rocket launch tubes. *J. Spacecraft Rockets,* 1988, 25(3), 209-16.
7. Kyoung-Ho, Kim & Keun-Shik, Chang. Three-dimensional structure of a supersonic jet impinging on an inclined piate. *J. Spacecraft Rockets,* 1994, 31(5), 736-44.